

Surface Tensions, Surface Potentials, and the Hofmeister Series of Electrolyte Solutions

Alexandre P. dos Santos,[†] Alexandre Diehl,[‡] and Yan Levin^{*†}[†]Instituto de Física, Universidade Federal do Rio Grande do Sul, Caixa Postal 15051, CEP 91501-970, Porto Alegre, RS, Brazil, and [‡]Departamento de Física, Instituto de Física e Matemática, Universidade Federal de Pelotas, Caixa Postal 354, CEP 96010-900, Pelotas, RS, Brazil

Received February 9, 2010. Revised Manuscript Received March 22, 2010

A theory is presented which allows us to accurately calculate the surface tensions and the surface potentials of electrolyte solutions. Both the ionic hydration and the polarizability are taken into account. We find a good correlation between the Jones–Dole viscosity B coefficient and the ionic hydration near the air–water interface. The kosmotropic anions such as fluoride, iodate, sulfate, and carbonate are found to be strongly hydrated and are repelled from the interface. The chaotropic anions such as perchlorate, iodide, chlorate, and bromide are found to be significantly adsorbed to the interface. Chloride and bromate anions become weakly hydrated in the interfacial region. The sequence of surface tensions and surface potentials is found to follow the Hofmeister ordering. The theory quantitatively accounts for the surface tensions of 10 sodium salts for which there is experimental data.

Introduction

Electrolyte solutions have been the subject of intense study for over a century. While the bulk properties of electrolytes are now quite well understood, their behavior at interfaces and surfaces still remains a puzzle. Over 100 years ago, Hofmeister observed that presence of electrolyte in water modified significantly the solubility of proteins. While some salts lead to protein precipitation (salting out), other salts stabilize proteins, increasing their solubility (salting in). A few years after this curious observation, Heydweiller¹ discovered that salt dissolved in water increased the surface tension of the solution–air interface. While cations had only a small influence on the surface tension, anions affected it quite significantly. Furthermore, the magnitude of the variation of the surface tension followed the same sequence discovered by Hofmeister earlier. It appeared that the two effects were related.

Because of its great importance for biology, over the past century there has been a tremendous effort to understand the ionic specificity. Since the air–water interface is relative simple, as compared to proteins, most of the theoretical work has concentrated on it. Langmuir² was the first to attempt a theoretical explanation of the physical mechanism behind the increase of the surface tension produced by electrolytes. Using the Gibbs adsorption isotherm equation, Langmuir concluded that the phenomenon was a consequence of ion depletion near the air–water interface and suggested that the depleted layer was about 4 Å in width. No clear explanation for existence of this ion-free layer was provided by Langmuir, and soon it became clear that in order to obtain a reasonable agreement with experiments, its width had to be a function of ionic concentration.³ A further insight was provided by Wagner,⁴ based on the Debye–Hückel (DH) theory of strong electrolytes.⁵ Wagner argued that ionic depletion was a consequence of the electrostatic repulsion produced by

the interaction of ions with their electrostatic images across the air–water interface. Wagner's theory was quite complicated, and a simplified version was proposed by Onsager and Samaras (OS), who also derived a limiting law which, they argued, had a universal validity for all electrolytes at sufficiently low concentrations.⁶ Indeed, careful experimental measurements have confirmed the OS limiting law.⁷ However at larger concentrations, OS theory was found to strongly underestimate surface tensions. It should be noted, however, that the quantitative measurements of surface tensions are very difficult, and there are some variation in the values reported by different experimental groups.⁸

Similar to Langmuir, Wagner and OS integrated the Gibbs adsorption isotherm equation to obtain the excess surface tension. Some time ago, Levin and Flores-Mena (LFM) proposed a different approach based on the direct Helmholtz free energy calculation.⁹ The LFM theory combined Langmuir, Wagner, and OS insights into one theory. They argued that, in addition to the ion-image interaction, ionic hydration leads to a hard-core-like repulsion from the Gibbs dividing surface. Using a 2 Å hydrated radius of Na^+ and Cl^- , they were able to obtain a very good agreement with the experimental measurements of surface tension of NaCl solution, up to 1 M concentration. However, the LFM theory failed to correctly account for the ionic specificity, predicting that the surface tension of NaI solution should be larger than that of NaCl, contrary to experiments. It was clear that the LFM theory was still lacking an important ingredient. An indication of the missing ingredient was already present in the work of Frumkin, 80 years earlier.¹⁰ Frumkin measured the electrostatic potential difference across the solution–air interface and found that for all halogen salts, except fluoride, the potential was lower in air than in water. This meant that anions were preferentially solvated near the interface. Boström et al.¹¹

*To whom correspondence should be addressed. E-mail: levin@if.ufrgs.br.

(1) Heydweiller, A. *Ann. Phys. (Leipzig)* **1910**, *33*, 145.
(2) Langmuir, I. *J. Am. Chem. Soc.* **1917**, *39*, 1848.
(3) (a) Harkins, W. D.; McLaughlin, H. M. *J. Am. Chem. Soc.* **1925**, *47*, 2083.
(b) Harkins, W. D.; Gilbert, E. C. *J. Am. Chem. Soc.* **1926**, *48*, 604.
(4) Wagner, C. *Phys. Z.* **1924**, *25*, 474.
(5) Debye, P. W.; Hückel, E. *Phys. Z.* **1923**, *24*, 185.

(6) Onsager, L.; Samaras, N. N. T. *J. Chem. Phys.* **1934**, *2*, 528.

(7) (a) Long, F. A.; Nutting, G. C. *J. Am. Chem. Soc.* **1942**, *64*, 2476. (b) Passoth, G. *Z. Phys. Chem. (Leipzig)* **1959**, *211*, 129.

(8) Henry, C. L.; Dalton, C. N.; Scruton, L.; Craig, V. S. *J. Phys. Chem. C* **2007**, *111*, 1015.

(9) Levin, Y.; Flores-Mena, J. E. *Europhys. Lett.* **2001**, *56*, 187.

(10) Frumkin, A. *Z. Phys. Chem. (Munich)* **1924**, *109*, 34.

(11) Boström, M.; Williams, D. R. M.; Ninham, B. W. *Langmuir* **2001**, *17*, 4475.

suggested that this ionic specificity was a consequence of dispersion forces arising from finite frequency electromagnetic fluctuations.¹² Their theory, however, predicted surface potentials of opposite sign to the ones measured by Frumkin, implying that cations were preferentially adsorbed to the interface. This was clearly contradicted by the simulations on small water clusters¹³ as well as by the subsequent large scale polarizable force fields simulations¹⁴ and by the photoelectron emission experiments.¹⁵ All these agreed with Frumkin that large anions, and not small cations, are preferentially solvated near the air–water interface. A theoretical explanation for this behavior was advanced by Levin,¹⁶ who argued that anionic surface solvation was a consequence of the competition between the cavitation and the electrostatic energies. The cavitation energy arises from the perturbation to the hydrogen bond network produced by ionic solvation. This results in a short-range force which drives ions toward the interface. This is counterbalanced by the electrostatic Born solvation force which arises from the dipolar screening of the ionic self-energy in aqueous environment. For hard (weakly polarizable) ions, the Born energy is much larger than the cavitation energy, favoring the bulk solvation. However for large polarizable ions, the energy balance is shifted. For such ions, ionic charge can easily redistribute itself so that even if a large fraction of ionic volume is exposed to air, the electrostatic energy penalty for this remains small, since most of the ionic charge remains hydrated. This means that through surface solvation large, strongly polarizable ions can have the best of two worlds—gain the cavitation energy at a small price in electrostatic self-energy. Levin derived the interaction potential quantifying this effect.¹⁶ In a follow-up paper, Levin et al.¹⁷ used this potential to quantitatively account for the surface tensions of all sodium halide salts. In this paper we will extend the theory of ref 17 to calculate the surface tensions and the surface potentials of others sodium salts and to derive the Hofmeister series.

Model and Theory

Consider an electrolyte solution confined to a mesoscopic drop of water of radius R , which corresponds to the position of the Gibbs dividing surface (GDS).^{17,18} We define the adsorption (ion excess per unit area) as

$$\Gamma_{\pm} = \frac{1}{4\pi R^2} \left[\int_0^{\infty} \rho_{\pm}(r) 4\pi r^2 dr - \frac{4\pi R^3}{3} c_b \right] \quad (1)$$

where $\rho_{\pm}(r)$ are the ionic density profiles and $c_b = \rho_+(0) = \rho_-(0)$ is the bulk concentration of electrolyte. If N ion pairs are inside the drop, eq 1 simplifies to $\Gamma_{\pm} = N/4\pi R^2 - c_b R/3$.

The water and air will be treated as uniform dielectrics of permittivities $\epsilon_w = 80$ and $\epsilon_a = 1$, respectively, with a discontinuity across the GDS. Clearly this is an approximation, the

validity of which can only be tested *a posteriori*. We note, however, that at any given instant an ion adsorbed to the interface will see it as almost flat—i.e. interface fluctuates, but the ion moves along with it. The dielectric environment seen by the ion at any instant should, therefore, be well approximated by a jump in the dielectric constant.

The surface tension can be obtained by integrating the Gibbs adsorption isotherm equation, $d\gamma = -\Gamma_+ d\mu_+ - \Gamma_- d\mu_-$, where μ_{\pm} are the chemical potentials of cations and anions, respectively. Let us first consider alkali-metal cations, such as lithium, sodium, or potassium. Because these cations are small, they have large surface charge density, which leads to strong interaction with surrounding water molecules, resulting in an effective hydrated radius a_h . We can, therefore, model these ions as hard spheres of radius a_h with a point charge q located at the origin. Because of their strong hydration, these cations cannot move across the GDS since this would require them to shed their solvation sheath. For mesoscopic drops we can neglect the curvature of the GDS. To bring a cation from bulk electrolyte to some distance $z > a_h$ from the GDS requires^{9,17}

$$W(z; a_h) = \frac{q^2}{2\epsilon_w} \int_0^{\infty} dk e^{-2s(z-a_h)} \frac{k[s \cosh(ka_h) - k \sinh(ka_h)]}{s[s \cosh(ka_h) + k \sinh(ka_h)]} \quad (2)$$

of work. The GDS is located at $z = 0$, and the axis is oriented into the drop. We have defined $s = (\kappa^2 + k^2)^{1/2}$, where $\kappa = (8\pi q^2 c_b / \epsilon_w k_B T)^{1/2}$ is the inverse Debye length. Equation 2 is well approximated by

$$W_{\text{ap}}(z; a_h) = \frac{W(a_h; a_h) a_h}{z} e^{-2k(z-a_h)} \quad (3)$$

(Supporting Information, Figure S1). This form will be used later to speed up the numerical calculations.

Unlike small cations, large halogen anions of bare radius a_0 have low electronic charge density and are weakly hydrated. The polarizability of an anion is γ_a , and we define its relative polarizability as $\alpha = \gamma_a/a_0^3$. We can model these ions as imperfect spherical conductors. When an anion is far from the interface, its charge $-q$ is uniformly distributed over its surface. However, when an anion begins to cross the GDS, its charge starts to redistribute itself on the surface so as to leave most of it in the high dielectric environment.¹⁶ The fraction of charge x which remains hydrated when the ionic center is at distance z from the GDS is determined by the minimization of the polarization energy¹⁶

$$U_p(z, x) = \frac{q^2}{2a_0\epsilon_w} \left[\frac{\pi x^2}{\theta(z)} + \frac{\pi[1-x]^2\epsilon_w}{[\pi - \theta(z)]\epsilon_0} \right] + \frac{g}{\beta} \left[x - \frac{1 - \cos[\theta(z)]}{2} \right]^2 \quad (4)$$

where $\theta(z) = \arccos[-z/a_0]$ and $g = (1 - \alpha)/\alpha$. We find

$$x(z) = \left[\frac{\lambda_B \pi \epsilon_w}{a_0 \epsilon_0 [\pi - \theta(z)]} + g[1 - \cos[\theta(z)]] \right] / \left[\frac{\lambda_B \pi}{a_0 \theta(z)} + \frac{\lambda_B \pi \epsilon_w}{a_0 \epsilon_0 [\pi - \theta(z)]} + 2g \right] \quad (5)$$

Substituting this back into eq 4, we obtain the polarization potential. This potential is repulsive, favoring ions to move toward the bulk. Nevertheless, the repulsion is quite soft compared to a hard-core-like repulsion of strongly hydrated cations. The force that drives anions toward the interface arises from cavitation. When ion is dissolved in water, it creates a cavity from

(12) Manciu, M.; Ruckenstein, E. *J. Phys. Chem. B* **2004**, *108*, 20479.

(13) (a) Perera, L.; Berkowitz, M. L. *J. Chem. Phys.* **1991**, *95*, 1954. (b) Dang, L. X.; Smith, D. E. *J. Chem. Phys.* **1993**, *99*, 6950. (c) Stuart, S. J.; Berne, B. J. *J. Phys. Chem. A* **1999**, *103*, 10300.

(14) (a) Jungwirth, P.; Tobias, D. J. *J. Phys. Chem. B* **2002**, *106*, 6361. (b) Jungwirth, P.; Tobias, D. J. *Chem. Rev.* **2006**, *106*, 1259. (c) Horinek, D.; Herz, A.; Vrbka, L.; Sedlmeier, F.; Mamatkulov, S. I.; Netz, R. R. *Chem. Phys. Lett.* **2009**, *479*, 173. (d) Brown, M. A.; D'Auria, R.; Kuo, I. F. W.; Krisch, M. J.; Starr, D. E.; Blum, H.; Tobias, D. J.; Hemminger, J. C. *Phys. Chem. Chem. Phys.* **2008**, *10*, 4778.

(15) (a) Markovich, G.; Pollack, S.; Giniger, R.; Cheshnovski, O. *J. Chem. Phys.* **1991**, *95*, 9416. (b) Ghosal, S.; Hemminger, J.; Blum, H.; Mun, B.; Hebenstreit, E. L. D.; Ketteler, G.; Ogleter, D. F.; Requejo, F. G.; Salmeron, M. *Science* **2005**, *307*, 563. (c) Garrett, B. *Science* **2004**, *303*, 1146.

(16) Levin, Y. *Phys. Rev. Lett.* **2009**, *102*, 147803.

(17) Levin, Y.; dos Santos, A. P.; Diehl, A. *Phys. Rev. Lett.* **2009**, *103*, 257802.

(18) Ho, C. H.; Tsao, H. K.; Sheng, Y. J. *J. Chem. Phys.* **2003**, *119*, 2369.

which water molecules are expelled. This leads to a perturbation to the hydrogen bond network and an energetic cost. For small voids, the cavitation energy scales with their volume.¹⁹ As ion moves across the interface, the cavity that it creates in water diminishes proportionally to the fraction of the volume exposed to air,^{16,17} producing a short-range interaction potential that forces it to move across the GDS

$$U_{\text{cav}}(z) = \begin{cases} \nu a_0^3 & \text{for } z \geq a_0 \\ \frac{1}{4} \nu a_0^3 \left(\frac{z}{a_0} + 1 \right)^2 \left(2 - \frac{z}{a_0} \right) & \text{for } -a_0 < z < a_0 \end{cases} \quad (6)$$

where $\nu \approx 0.3k_B T/\text{\AA}^3$ is obtained from bulk simulations.²⁰ For small strongly hydrated cations, this energy gain does not compensate for the electrostatic energy penalty of exposing the ionic charge to the low dielectric environment. For large polarizable ions, on the other hand, electrostatic energy penalty is small, and the cavitation energy is sufficient to favor the surface solvation. The total potential felt by an unhydrated anion is then¹⁷

$$U_{\text{tot}}(z) = \begin{cases} W(z; a_0) + \nu a_0^3 + \frac{q^2}{2\epsilon_w a_0} & \text{for } z \geq a_0 \\ W(a_0; a_0)z/a_0 + U_p(z) + U_{\text{cav}}(z) & \text{for } 0 < z < a_0 \\ U_p(z) + U_{\text{cav}}(z) & \text{for } -a_0 < z \leq 0 \end{cases} \quad (7)$$

The density profiles can now be calculated by integrating the nonlinear modified Poisson–Boltzmann equation (mPB):

$$\begin{aligned} \nabla^2 \phi(r) &= -\frac{4\pi q}{\epsilon_w} [\rho_+(r) - \rho_-(r)] \\ \rho_+(r) &= \frac{N\Theta(R - a_h - r)e^{-\beta q\phi(r) - \beta W(z; a_h)}}{\int_0^{R - a_h} 4\pi r^2 dr e^{-\beta q\phi(r) - \beta W(z; a_h)}} \\ \rho_-(r) &= \frac{N e^{\beta q\phi(r) - \beta U_{\text{tot}}(r)}}{\int_0^{R + a_0} 4\pi r^2 dr e^{\beta q\phi(r) - \beta U_{\text{tot}}(r)}} \end{aligned} \quad (8)$$

where $\beta = 1/k_B T$ and Θ is the Heaviside step function. The boundary condition for this mPB equation is vanishing of the electrostatic potential and of electric field at $R + a_0$. To speed up the numerical calculations, we can replace $W \rightarrow W_{\text{ap}}$.

Sodium–Halogen Salts

First, we study the sodium–halogen salts.¹⁷ The anion radii were obtained by Latimer, Pitzer, and Slansky²¹ by fitting the experimentally measured free energies of hydration to the Born model. Since our theory in the bulk also reduces to the Born model, these radii are particularly appropriate: $a_{\text{I}} = 2.26 \text{ \AA}$, $a_{\text{Br}} = 2.05 \text{ \AA}$, $a_{\text{Cl}} = 1.91 \text{ \AA}$, and $a_{\text{F}} = 1.46 \text{ \AA}$. For ionic polarizabilities we use the values from ref 22: $\gamma_{\text{I}} = 7.4 \text{ \AA}^3$, $\gamma_{\text{Br}} = 5.07 \text{ \AA}^3$, $\gamma_{\text{Cl}} = 3.77 \text{ \AA}^3$, and $\gamma_{\text{F}} = 1.31 \text{ \AA}^3$. We should note that in simulations the values of ionic polarizability are sometimes artificially lowered to avoid the polarization catastrophe. This catastrophe is a consequence of the truncation of the multipole expansion at the dipolar level. Since the calculations presented in

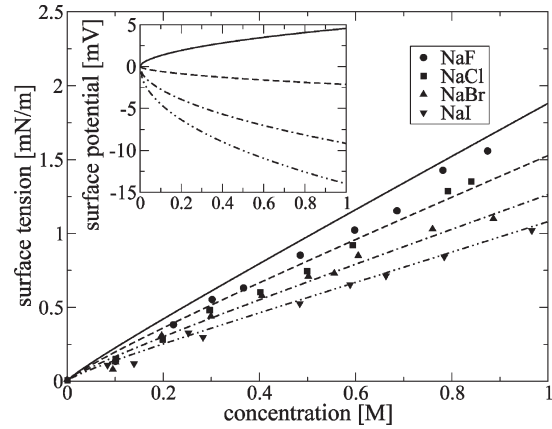


Figure 1. Excess surface tensions of NaF, NaCl, NaBr, and NaI solutions. The symbols are the experimental data,^{23–25} and the lines are the results of the present theory. The inset shows the surface potential difference as a function of molar concentration.

this work are nonperturbative, there is no need to artificially lower the polarizabilities.

The excess surface tension can be obtained by integrating the Gibbs adsorption isotherm equation (eq 1). At the level of PB approximation the chemical potential that enters into equation (eq 1) is simply that of an ideal gas, $\beta\mu_{\pm} = \ln(c_{\pm}\Lambda_{\pm}^3)$, where Λ_{\pm} are the de Broglie thermal wavelengths. Comparing to more sophisticated theories and simulations, we find that this approximation works quite well up to fairly large concentrations $\approx 1 \text{ M}$.^{9,18} We start with NaI. Since I^- is large and soft, it should be unhydrated in the interfacial region. Adjusting the hydrated radius of Na^+ to best fit the experimental data²³ for NaI, we obtain¹⁷ $a_{\text{h,Na}} = 2.5 \text{ \AA}$. We will use this partially hydrated radius of Na^+ in the rest of the paper. Considering that Br^- is also large and soft, we expect that it will also remain unhydrated in the interfacial region. This expectation is well justified, and we obtain a very good agreement with the experimental data²⁵ (see Figure 1). For F^- the situation should be very different. This ion is small, hard, and strongly hydrated. This means that, just like for a cation, a hard-core repulsion from the GDS must be explicitly included in the mPB equation. For hydrated (or partially hydrated) anions the density is then

$$\rho_-(r) = \frac{N\Theta(R - a_h - r)e^{\beta q\phi(r) - \beta W(z; a_h)}}{\int_0^{R - a_h} 4\pi r^2 dr e^{\beta q\phi(r) - \beta W(z; a_h)}} \quad (9)$$

In this case, the mPB boundary condition becomes vanishing of the potential and of electric field at $r = R - a_{\text{h},<}$, where $a_{\text{h},<}$ is the smaller of the cation and anion radii. Using this in eq 8, a very good agreement with the experimental data²³ is found for NaF, using the usual bulk hydrated radius of F^- , $a_{\text{h,F}} = 3.52 \text{ \AA}$ ²⁶ (see Figure 1). The table salt, NaCl, is the most difficult case to study theoretically, since Cl^- is sufficiently small to remain partially hydrated near the GDS. We find a good fit to the experimental data²⁴ (Figure 1) using a partially hydrated radius of Cl^- , $a_{\text{h,Cl}} = 2.0 \text{ \AA}$, which is very close to its bare size.

In Supporting Information Figure S2, we present the ionic density profiles for these salts. In agreement with the polarizable

(19) (a) Lum, K.; Chandler, D.; Weeks, J. D. *J. Phys. Chem. B* **1999**, *103*, 4570. (b) Chandler, D. *Nature (London)* **2005**, *437*, 640.

(20) Rajamani, S.; Truskett, T. M.; Garde, S. *Proc. Natl. Acad. Sci. U.S.A.* **2005**, *102*, 9475.

(21) Latimer, W. M.; Pitzer, K. S.; Slansky, C. M. *J. Chem. Phys.* **1939**, *7*, 108.

(22) Pyper, N. C.; Pike, C. G.; Edwards, P. P. *Mol. Phys.* **1992**, *76*, 353.

(23) Matubayasi, N.; Tsunemoto, K.; Sato, I.; Akizuki, R.; Morishita, T.; Matuzawa, A.; Natsukari, Y. *J. Colloid Interface Sci.* **2001**, *243*, 444.

(24) Matubayasi, N.; Matsuo, H.; Yamamoto, K.; Yamaguchi, S.; Matuzawa, A. *J. Colloid Interface Sci.* **1999**, *209*, 398.

(25) Matubayasi, N., unpublished.

(26) Nightingale, E. R., Jr. *J. Phys. Chem.* **1959**, *63*, 1381.

Table 1. Surface Potentials Difference at 1 M for Various Salts

	calculated (mV)	Frumkin ^{10,29} (mV)	Jarvis et al. ³⁰ (mV)
NaF	4.7		
NaCl	-2.1	-1	≈-1
NaBr	-9.4		≈-5
NaI	-14.3	-39	≈-21
NaIO ₃	5		
NaBrO ₃	-0.12		
NaNO ₃	-8.27	-17	≈-8
NaClO ₃	-11.02	-41	
NaClO ₄	-31.1	-57	
Na ₂ CO ₃	10.54	3	≈6
Na ₂ SO ₄	10.17	3	≈35

force fields simulations,^{13,14,27} the large halogens I⁻ and Br⁻ are adsorbed at the interface. However, contrary to these simulations and in agreement with the vibrational sum-frequency spectroscopy,²⁸ their concentration at the GDS remains below that in the bulk. Surprisingly, the simulations predict so much adsorption that the surface tension of the electrolyte solutions becomes negative,²⁷ contrary to experiments. This might again be a consequence of the breakdown of the multipole expansion implicit in the polarizable force fields simulations.

The electrostatic potential difference across the air–water interface is $\chi = \phi(\infty) - \phi(0)$. Experimental measurements of the surface potential are very difficult, and there is a significant variation in the values reported in the literature. However, if we take the difference between various measurements as a possible indication of error bars, our results are in reasonable agreement with the measurements of Frumkin^{10,29} and Jarvis et al.³⁰ (Table 1).

Oxy Anion Salts

We next study the surface potentials and the surface tensions of sodium salts with more complex anions, such as chlorate, nitrate, bromate, iodate, perchlorate, sulfate, and carbonate. Naively one might expect that because of their large size, these oxy anions will lose their hydration sheath near the GDS. This, however, is not necessarily the case. At the moment there is no reliable theory of hydration; nevertheless, it has been known for a long time that ions can be divided into two categories: structure-makers (kosmotropes) and structure-breakers (chaotropes). This dichotomy is reflected, for example, in the Jones–Dole viscosity B coefficient. It is found experimentally that for large dilutions viscosity varies with the concentration of electrolyte as³¹

$$\eta_r = 1 + A\rho^{1/2} + B\rho \quad (10)$$

where A is a positive constant, resulting from the ion–ion interactions, and B is related to the ion–solvent interactions. For kosmotropes B coefficient is positive, while for chaotropes it is negative (see Table 2). In particular, we observe that F⁻ is a kosmotrope, while Br⁻ and I⁻ are chaotropes. Chloride ion appears to be on the borderline between the two regimes. The classification of ions into kosmotropes and chaotropes correlates well with our theory of surface tensions of halogen salts—kosmotropes were found to remain strongly hydrated near the GDS, while chaotropes lost their hydration sheath near the interface. It is curious that the bulk dynamics of ion–water

Table 2. B Coefficients for Various Ions³¹

ions	B coefficient	ions	B coefficient
Na ⁺	0.085	BrO ₃ ⁻	0.009
F ⁻	0.107	NO ₃ ⁻	-0.043
Cl ⁻	-0.005	ClO ₃ ⁻	-0.022
Br ⁻	-0.033	ClO ₄ ⁻	-0.058
I ⁻	-0.073	CO ₃ ²⁻	0.294
IO ₃ ⁻	0.140	SO ₄ ²⁻	0.206

interaction, measured by the value of the viscosity B coefficient, is so strongly correlated with the statics of ionic hydration, measured by the surface tension of electrolyte solutions.

It is reasonable, then, to suppose that the classification of ions into chaotropes and kosmotropes, based on their B coefficient, will also extend to more complicated ions as well. Thus, we expect that chaotropes NO₃⁻, ClO₃⁻, and ClO₄⁻ will lose their hydration sheath near the GDS, while the kosmotropes IO₃⁻, CO₃²⁻, and SO₄²⁻ will remain strongly hydrated. Furthermore, since B coefficients of these ions are large (as compared to F⁻), we expect that these ions will remain as hydrated near the GDS as they were in the bulk, similar to what was found for fluoride anion. On the other hand, the B coefficient of BrO₃⁻ is very close to zero, and similarly to Cl⁻, we expect bromate to be only very weakly hydrated near the GDS.

There is an additional difficulty with studying oxy anions. Since these ions are not spherically symmetric, their radius is not well-defined. Nevertheless, it has been observed that empirical radius

$$a_0 = \frac{n_{\text{oxy}}}{4}(d + 1.4 \text{ \AA}) \quad (11)$$

where d is the X–O covalent bond length in the corresponding salt crystal and n_{oxy} is the number of oxygens in anion, correlates very well with the experimental measurements of entropies of hydration.³² Using this formula, we calculate $a_{\text{NO}_3} = 1.98 \text{ \AA}$, $a_{\text{ClO}_3} = 2.16 \text{ \AA}$, and $a_{\text{ClO}_4} = 2.83 \text{ \AA}$ for the bare radius of the chaotropic oxy anions.

The polarizabilities of NO₃⁻ and ClO₄⁻ are given in ref 22: $\gamma_{\text{NO}_3} = 4.09 \text{ \AA}^3$ and $\gamma_{\text{ClO}_4} = 5.4 \text{ \AA}^3$. Unfortunately, this reference does not provide the polarizability of chlorate ion. However, since the polarizability is, in general, proportional to the volume of an ion, we can easily estimate it based on the polarizability of iodate, which is given in ref 22: $\gamma_{\text{IO}_3} = 8.0 \text{ \AA}^3$. We then obtain $\gamma_{\text{ClO}_3} = 5.3 \text{ \AA}^3$.

Using eq 8, we can now calculate the surface potential, the ionic density distribution (Supporting Information, Figure S3), and, integrating the Gibbs adsorption isotherm, the excess surface tension (Figures 2, 3, and 4). We stress that in all the calculations we are using the same value of sodium hydrated radius, $a_{\text{h,Na}} = 2.5 \text{ \AA}$, obtained for halogen salts. For chlorate and nitrate, the predictions of the theory are in good agreement with the experimental measurements of Matubayasi^{25,33} (see Figures 2 and 3).

For perchlorate, the theoretical surface tension is slightly lower than what was found experimentally (Figure 4). The difficulty is that since the cavitation energy scales with the volume of the ion, for large ions it becomes very sensitive to the precise value of the ionic radius. For example, if we use a slightly smaller radius of perchlorate $a_{\text{ClO}_4} = 2.75 \text{ \AA}$, we obtain a good agreement with experiment (Figure 4). The theory shows that ClO₄⁻ is adsorbed stronger than either ClO₃⁻ or I⁻ (Supporting Information, Figure S4). This conclusion is also in agreement with the simulations.³⁴

(27) (a) Ishiyama, T.; Morita, A. *J. Phys. Chem. C* **2007**, *111*, 721. (b) D'Auria, R.; Tobias, D. J. *J. Phys. Chem. A* **2009**, *113*, 7286.

(28) Raymond, E. A.; Richmond, G. L. *J. Phys. Chem. B* **2004**, *108*, 5051.

(29) Randles, J. E. B. *Advances in Electrochemistry and Electrochemical Engineering*; Interscience: New York, 1963; Vol. 3, p 1.

(30) Jarvis, N. L.; Scheiman, M. A. *J. Phys. Chem.* **1968**, *72*, 74.

(31) Jenkins, H. D. B.; Marcus, Y. *Chem. Rev.* **1995**, *95*, 2695.

(32) Couture, A. M.; Laidler, K. L. *Can. J. Chem.* **1957**, *35*, 202.

(33) Matubayasi, N.; Yoshikawa, R. *J. Colloid Interface Sci.* **2007**, *315*, 597.

(34) Ottoson, N.; Vacha, R.; Aziz, E. F.; Pokapanich, W.; Eberhardt, W.; Svensson, S.; Ohrwall, G.; Jungwirth, P.; Bjorneholm, O.; B. B. W. *J. Chem. Phys.* **2009**, *131*, 124706.

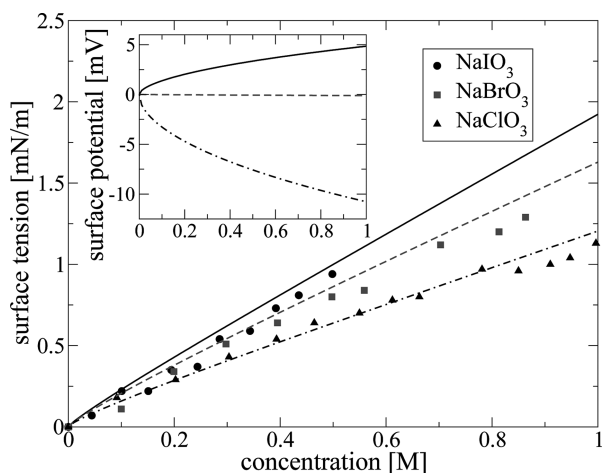


Figure 2. Excess surface tensions of NaIO_3 , NaBrO_3 , and NaClO_3 solutions. The symbols are experimental data,²⁵ and the lines are obtained using the present theory. The inset shows the electrostatic surface potential difference and has the same horizontal axis label as the main figure.

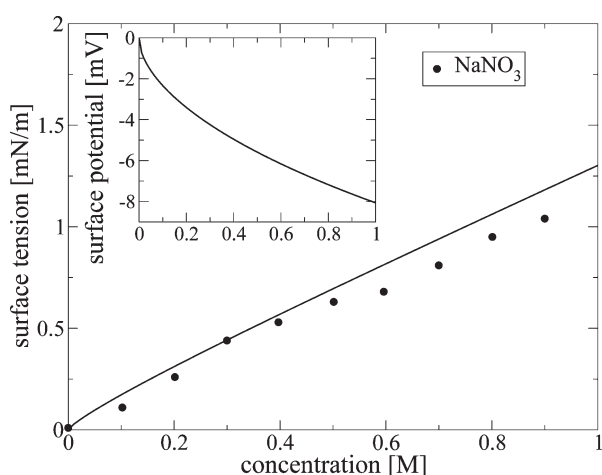


Figure 3. Excess surface tension of NaNO_3 solution. The symbols are the experimental data,³³ and the lines are the present theory. The inset shows the electrostatic surface potential difference vs the molar concentration.

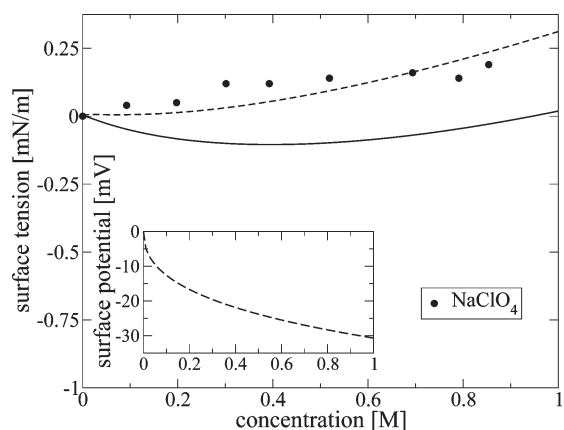


Figure 4. Excess surface tensions of NaClO_4 solution. The symbols are the experimental data,²⁵ and the lines are the present theory. The solid line is obtained using $a_{\text{ClO}_4} = 2.83 \text{ \AA}$ from eq 11 and the dashed line using $a_{\text{ClO}_4} = 2.75 \text{ \AA}$. The inset shows the electrostatic surface potential difference vs the molar concentration.

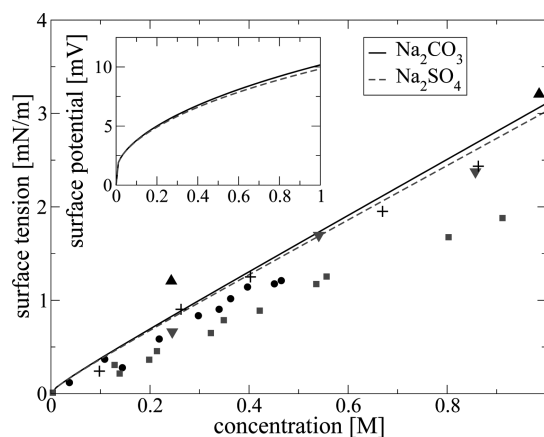


Figure 5. Excess surface tensions of Na_2CO_3 and Na_2SO_4 solutions. The circles and the squares are the experimental data for sodium carbonate and sodium sulfate, respectively.²³ The up and down triangles are the data of Jarvis and Scheiman.³⁰ The plus symbols are the data of Weissenborn and Pugh³⁵ for the Na_2SO_4 salt. The lines are the present theory. The inset shows the surface potential difference vs the molar concentration.

We next calculate the surface tension of sodium salts with kosmotropic anions. Since the B coefficient of iodate is so large, we expect that this ion will remain completely hydrated near the GDS. The bulk hydrated radius of IO_3^- is $a_{\text{h,IO}_3} = 3.74 \text{ \AA}$.³⁴ Using this in eq 9, we obtain an excellent agreement with the experimental data²⁵ (Figure 2). The B coefficient of bromate is almost zero, so that BrO_3^- should be only very weakly hydrated near the GDS. Indeed, using $a_{\text{h,BrO}_3} = 2.41 \text{ \AA}$, we obtain a very good agreement with the experimental data²⁵ (Figure 2). This value is only slightly above the crystallographic radius of BrO_3^- , $a_{\text{BrO}_3} = 2.31 \text{ \AA}$, obtained using eq 11.

Finally, we consider the surface tension of sodium salts with divalent anion. The predictions of the theory, in this case, should be taken with a grain of salt, since it is well-known that Poisson–Boltzmann theory begins to lose its validity for divalention as a result of interionic correlations.³⁶ Nevertheless, it is curious to see how well the theory does in this limiting case. The B coefficients of SO_4^{2-} and CO_3^{2-} are large and positive, so that we expect these ions to be fully hydrated, $a_{\text{h,SO}_4} = 3.79 \text{ \AA}$ and $a_{\text{h,CO}_3} = 3.94 \text{ \AA}$,²⁶ respectively. Calculating the surface tensions, we find that our results are somewhat above those measured by Matubayasi et al.²³ Curiously, the theory agrees well the measurements of Jarvis and Scheiman³⁰ and of Weissenborn and Pugh³⁵ (Figure 5). At this point we do not know what to make of this agreement. The surface potentials of sodium sulfate and sodium carbonate are listed in Table 1. In Supporting Information Table S1, we summarize the classification of all ions and the radii used in calculations.

Conclusions

We have presented a theory which allows us to quantitatively calculate the surface tensions and the surface potentials of 10 sodium salts with only one adjustable parameter, the partial hydrated radius of the sodium cation. We find that anions near the GDS can be classified into kosmotropes and chaotropes. Kosmotropes remain hydrated near the interface, while the chaotropes lose their hydration sheath. For all salts studied in this paper, the classification of ions into the structure-makers/breakers agrees with the bulk characterization based on the

(35) Weissenborn, P. K.; Pugh, R. J. *J. Colloid Interface Sci.* **1996**, *184*, 550.

(36) Levin, Y. *Rep. Prog. Phys.* **2002**, *65*, 1577.

Jones–Dole viscosity B coefficient. Unfortunately, for complex ions there is no *a priori* way to predict which ones will behave as kosmotropes or chaotropes. This information must be taken from independent experiments. If anions are arranged in the order of increasing electrostatic surface potential difference, we obtain the extended lyotropic (Hofmeister) series, $\text{CO}_3^{2-} > \text{SO}_4^{2-} > \text{IO}_3^- > \text{F}^- > \text{BrO}_3^- > \text{Cl}^- > \text{NO}_3^- > \text{Br}^- > \text{ClO}_3^- > \text{I}^- > \text{ClO}_4^-$. To our knowledge this is the first time that this sequence has been derived theoretically. The theory also helps to understand why the Hofmeister series is relevant to biology.³⁷ In general, proteins have both hydrophobic and hydrophilic moieties. If the hydrophobic region is sufficiently large, it can become completely dewetted,¹⁹ surrounded by a vapor-like film into which chaotropic anions can become adsorbed.³⁸ This will help to solvate proteins, but at the same time will destroy their tertiary structure, denaturing them in the process. On the other hand, the kosmotropic ions will favor protein precipitation. The action is again twofold. The kosmotropes adsorb water which could, otherwise, be used to solvate hydrophilic moieties. They also screen the electrostatic repulsion, allowing charged proteins to come

into a close contact and to stick together as the result of their van der Waals and hydrophobic interactions. This leads to formation of large clusters which can no longer be dispersed in water and must precipitate. Finally, contrary to previous suggestions,¹¹ the success of the present theory shows that dispersion forces do not play a significant role in determining the surface tension or the Hofmeister series of electrolyte solutions.

Acknowledgment. We thank Prof. Norihiro Matubayasi for providing us with the unpublished data for the surface tensions of chlorate, bromate, iodate, and perchlorate. Y.L. is also grateful to Dr. Delfi Bastos González for first bringing the kosmotropic nature of iodate to his attention. This work was partially supported by the CNPq, INCT-FCx, and by the US-AFOSR under grant FA9550-09-1-0283.

Supporting Information Available: Comparison between the exact expression (eq 2) and its approximation (eq 3); the ionic density profiles for all the electrolyte solutions discussed; and a summary showing ionic classification into chaotropes and kosmotropes and their effective radii. This material is available free of charge via the Internet at <http://pubs.acs.org>.

(37) (a) Collins, K. D.; Washanbaugh, M. W. *Q. Rev. Biophys.* **1985**, *18*, 323. (b) Zhang, Y.; Cremer, P. S. *Curr. Opin. Chem. Biol.* **2006**, *10*, 658. (c) Pegram, L. M.; Record, M. T. *J. Phys. Chem. B* **2007**, *111*, 5411.

(38) Huang, D. M.; Cottin-Bizonne, C.; Ybert, C.; Bocquet, L. *Phys. Rev. Lett.* **2007**, *98*, 177801.